

Original Article

Long noncoding RNA XIST participates hypoxia-induced angiogenesis in human brain microvascular endothelial cells through regulating miR-485/SOX7 axis

Chenggong Hu, Xue Bai, Chang Liu, Zhi Hu

Department of Critical Care Medicine, West China Hospital of Sichuan University, Chengdu 610041, Sichuan, China

Received July 17, 2019; Accepted August 17, 2019; Epub October 15, 2019; Published October 30, 2019

Abstract: Background: Long non-coding RNAs (lncRNAs) X-inactive specific transcript (XIST) has identified to involve into the tumor cell angiogenesis. However, whether XIST contributes to Human Brain Microvascular Endothelial Cells (HBMEC) angiogenesis as well as potential mechanisms are largely unclear. Methods: The expression of XIST, miR-485-3p and SRY-box 7 (SOX7) in HBMEC were altered by transfection. The cell viability, cell migration and tube formation of HBMEC were measured, respectively. The cross-regulations between XIST, miR-485-3p, SOX7, and vascular endothelial growth factor (VEGF) signaling pathway were investigated by RT-qPCR and Western blot assay. Results: In this study, we characterized the upregulation of XIST in HBMEC under hypoxia condition. Meanwhile, XIST silencing impaired hypoxia-induced cell proliferation, migration and tube formation. Besides, our integrated experiments identified that XIST may competitively bind with miR-485-3p and then modulate the derepression of downstream target SRY-box 7 (SOX7). Mechanically, knockdown of XIST impaired hypoxia-induced angiogenesis via miR-485-3p/SOX7 axis and subsequent suppression of VEGF signaling pathway. Conclusion: Altogether, the present study suggested that XIST is required to maintain VEGF signaling expression in HBMEC under hypoxia condition and plays a vital role in hypoxia-induced angiogenesis via miR-485-3p/SOX7 axis.

Keywords: Ischemic stroke, angiogenesis, XIST, miR-485-3p, SOX7

Introduction

Ischemic stroke is one of the major causes of death and disability worldwide and it occurs in absence of blood flow with oxygen and nutrients [1]. Although great improvements have been made in medical and endovascular recanalization therapy, therapeutic choices for ischemic stroke are still limited [2, 3]. As the body will undergo angiogenesis to restore blood flow when it lacks of blood flow, angiogenesis is essential for the repair of ischemic stroke. Therefore, the promotion of angiogenesis is considered as an effective therapeutic target of treatment of ischemic stroke [4]. A deeper understanding of the of angiogenesis after ischemic stroke will help to facilitate the arrival of such therapies.

Long non-coding RNAs (lncRNAs) emerges as a class of non-coding RNAs that are greater than 200 nucleotides in length and participate in

various biological processes. lncRNAs play a vital role in the development of brain disease and targeting whom could effectively reverse the progress of brain tumors [5], cerebral hemorrhage [6], as well as ischemic stroke [7]. Recently, emerging evidence suggested that lncRNAs are aberrantly expressed and play important roles in the process of angiogenesis after ischemic stroke [8]. For example, lncRNA HIF1A-AS2 was identified as an angiogenic factor by upregulating of HIF-1 α by sponging to miR-153-3p in human umbilical vein endothelial cells in hypoxia [9]. In addition, another lncRNA SNHG12 was found to promote angiogenesis in brain microvascular endothelial cells exposure to oxygen-glucose deprivation/reoxygenation [10]. Nevertheless, up to date, only limited number of lncRNAs have been studied for their effects of the angiogenesis after ischemic stroke and further studies are quite needed to demonstrate lncRNA functions.

XIST participate in hypoxia-induced angiogenesis

The lncRNA X-inactive specific transcript (XIST), a product of the XIST gene, is [11] dysregulated in several cancers and is involved in tumor cell invasion, progression, metastasis, and poor prognosis [11-13]. XIST also plays a role in cell proliferation, differentiation, and genome maintenance [14]. Neumann et al. identified that XIST was increased in human umbilical vein endothelial cells under hypoxia stimulation [15] and XIST silencing promoted the cell proliferation, attenuated cell apoptosis in ox-LDL-induced endothelial cells [16]. Additionally, a recent study identified that knockdown of XIST could increase blood-tumor barrier permeability and inhibit glioma angiogenesis by directly regulating miR-137 [17]. However, the exact expression, function, and mechanism of XIST in ischemic stroke remain uncovered.

In this study, we determined the expression levels of XIST in Human Brain Microvascular Endothelial Cells (HBMEC) under hypoxia condition and further investigated the effects of exogenous regulation of XIST on HBMEC angiogenesis. We found that knockdown of XIST could affect hypoxia-induced angiogenesis via regulation of miR-485-3p/SOX7/VEGF axis. The results of our study would provide more evidence about the involvement of lncRNAs in angiogenesis after ischemic stroke and provide a promising treatment strategy for this disease.

Materials and methods

Cell culture

HBMEC were obtained from Sciencell (Carlsbad, CA, USA). The Endothelial Cell Medium (ECM, Sciencell) with 10% fetal bovine serum (FBS; Hyclone, Logan, UT, USA) was used for cell culture. Human embryonic kidney (HEK) 293T cells (Cell Bank of the Chinese Academy of Sciences, Shanghai, China) were maintained in Dulbecco's Modified Eagle Medium (DMEM; Gibco, Grand Island, NY, USA) with 10% FBS. Normally, Cells were maintained in an incubator filled with 95% air and 5% CO₂ at 37°C. For hypoxia treatment, HBMEC were incubated in a hypoxic incubator filled with 94% N₂, 5% CO₂, and 1% O₂ at 37°C.

Cell transfection

The small interfering RNA (siRNA) targeting XIST (si-XIST) and negative control (si-NC) scramble siRNA was designed and constructed by

RiboBio Co. (Guangzhou, China). Sequence: si-XIST#1 (5'-TGTCTCTTTCTTTCTTGCTTTGCT-3'), si-XIST#2 (5'-TCTCTTTCTTTCTTGCTTTGCTCT-3'), si-NC (5'-TCTATCTAGTAAATTCTGCCGTCAT-3'). The miR-485-3p mimics, negative control mimics (miR-NC) and miR-485-3p inhibitors, inhibitors control were also purchased from RiboBio Co. For cell transfection, HBMEC were cultured in 96-well plates at a density of 5000 cells per well and transfected with siRNAs (si-XIST1, si-XIST2, si-NC), miR-485-3p mimics, miR-NC, miR-485-3p inhibitors and inhibitors control at final concentrations of 10 and 20 nM, respectively, together with 3 µL Lipofectamine 2000 reagent (Invitrogen) in accordance with the manufacturer's protocol. Overexpression of SOX7 were achieved by transfected with pcDNA3.1-SOX7 (pcDNA3.1 empty vector was acted as scramble control and named vector, obtained from GenePharma Company, Shanghai, China). The cells in each well were transfected with pcDNA3.1-SOX7 or empty vector with Lipofectamine 2000. After 48 h of transfection, the cells were collected and used for further analysis.

Cell viability

Cell viability was measured by CCK-8 assay (Sigma-Aldrich, St. Louis, MO, USA). In brief, approximately 5×10³ cells were planted into a 96-well plate. After transfection, the culture medium was replaced by 100 µl ECM containing 10 µl CCK8 solution. After incubated at 37°C for 2 h, the absorbance at 570 nm was detected on a Microplate Reader (Bio-Rad, Hercules, CA, USA). All experiments were carried out in triplicate.

Wound healing assay

When cells grew around 70~80% confluence in wells, scratch the bottom of the well with a 200 µl pipette tip to create a linear region void of cells. After we removed the supernatant cells and washed with PBS, cells were treated with indicated treatment and the images of the denuded zone were recorded with the inverted microscope (Olympus, Japan) at 0 and 24 h, respectively. Data were representative of three individual experiments.

Cell migration

Cell migration was analyzed using Transwell chambers (8 µm, BD Biosciences, Bedford, MA, USA). Cells from the different groups were plat-

XIST participate in hypoxia-induced angiogenesis

ed in the upper chambers at a density of 2×10^4 /well in serum-free medium. Next, 500 μ L of ECM with 10% FBS was added to the lower chambers. After 24 h, the cells on the upper surface were softly removed. Migrated cells were fixed in 4% paraformaldehyde (Sigma), stained with 1% crystal violet (Sigma), and counted under an optical microscope ($\times 100$ magnification). Cell counts are expressed as the mean number of cells from five random fields per filter.

Angiogenesis assay

For detection of angiogenic capacity, HBMEC were harvested and seeded in Matrigel-coated 96-well plates (BD Biosciences) at a density of 5×10^3 /well and incubated in normal condition. After different treatment for 24 h, the cells were observed after another 4 h and tube formation was visualized and photographed with a phase contrast inverted microscope at $100\times$ magnification. Quantification of the length of closed structures was performed using Image J with the Angiogenesis Analyzer plugin¹⁶.

Real-time quantitative PCR

Total RNA was extracted from the HBMEC by using TRIzol reagent (Invitrogen, Carlsbad, CA, USA) following the manufacturer's protocol. The purity of the RNA was determined and the reverse transcription (PrimeScript™ RT reagent Kit) and real-time quantitative PCR (SYBR Premix Ex Taq II) were performed in accordance with the kit instructions (Takara Biotechnology Co., Ltd., China). The following primers were used: XIST F, 5'-CAGACGTGTGCTCTTC-3' and R, 5'-CGATCTGTAAGTCCACCA-3'; SOX7 F, 5'-GCCACCTACCACTCCACT-3' and R, 5'-GACGGCTCCTCTGCCACTCAA-3'; β -actin F, 5'-GGCACCACACCTTCTACAAT-3' and R, 5'-GTGGTGTTGAA-GCTGTAGCC-3'; U6 F, 5'-CTCGCTTCGGCAGCA-CA-3' and R, 5'-AACGCTTCACGAATTTGCGT-3'. The relative amount was calculated using the $2^{-\Delta\Delta Ct}$ method as previously described [18].

Luciferase reporter assay

The XIST fragment containing putative miR-485-3p binding site was cloned into a pmirGlo vector (Promega, USA), namely XIST WT. Mutation of the putative miR-485-3p target sequences in the 3-UTR of XIST was generated

with the site-directed gene mutagenesis kit (Takara), namely XIST-MUT. The two reporter plasmids, as well as empty vector plasmid were co-transfected with miR mimics or miR-NC into 293T cells. For miR-485-3p and SOX7 interaction, the putative and mutated miR-485-3p target binding sequence in SOX7 were synthesized and cells were co-transfected with WT or Mut SOX7 reporter gene plasmid or pmirGlo plasmids via Lipofectamine 2000. At 48 h post-transfection, cells were harvested, and the firefly luciferase activity was measured by a dual-luciferase reporter assay system (Promega) and normalized to with Renilla luciferase activities.

Western blot

After the indicated treatment, HBMEC were collected and lysed in RIPA Lysis and Extraction Buffer (Thermo Fisher Scientific, Waltham, MA, USA). Protein concentrations were evaluated by the BCA method (Micro BCA Protein Assay Kit, Thermo Fisher Scientific) and 50 μ g of each sample were separated by SDS-PAGE on a 12% gel. Then the proteins were transferred to PVDF membranes (Millipore, MA, USA) and the membranes were blocked with 5% skim milk. The blots were then incubated with the SOX7 (ab220293), vascular endothelial growth factor (VEGFR2; ab2349), vascular endothelial growth factor A (VEGFA; ab1316), ERK (ab17942), p-ERK (ab50011), Akt (ab8805), p-Akt (ab38449) and β -actin (ab8226, all obtained from Abcam) overnight at 4°C. Subsequently, the membranes were probed with horseradish peroxidase-conjugated secondary antibodies at room temperature for 1 h. The bands were visualized with an enhanced chemiluminescence system (Pierce, Rockford, IL, USA) and protein intensity were normalized to β -actin.

Statistics

Values were expressed as the mean \pm standard deviation for each group and statistical tests were carried out with GraphPad Prism 6.0 software (San Diego, CA, USA). Student's t-test was performed for comparisons between two groups, and one-way analysis of variance followed by Tukey's post hoc test was used among multiple groups. Statistically significant was considered $P < 0.05$.

XIST participate in hypoxia-induced angiogenesis

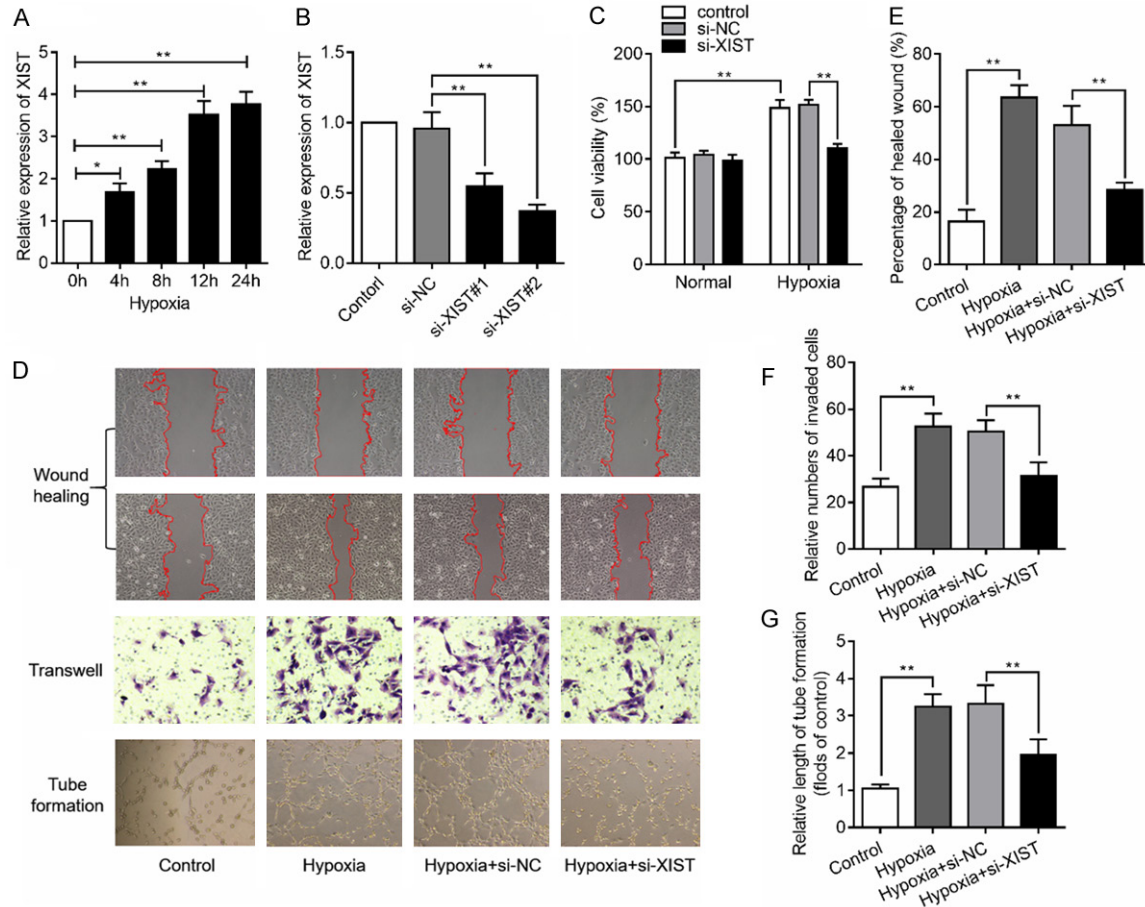


Figure 1. LncRNA XIST silencing impairs hypoxia-induced angiogenesis in HBMEC. (A) Relative expression levels of XIST were measured in HBMEC under hypoxia stimulation for various time. (B) XIST expression levels in the HBMEC transfected with specific XIST siRNAs (si-XIST#1, and si-XIST#2) or siRNA negative control (si-NC) were detected by RT-qPCR assay. (C) Cell proliferation was detected in HBMEC transfected with si-NC or si-XIST under normal or hypoxia condition. (D) HBMEC were stimulated with hypoxia followed by transfection with si-XIST or si-NC, cells were then subjected to wound healing assay (E), transwell assay (F) and tube formation assay (G). * $P < 0.05$, ** $P < 0.01$.

Results

Knockdown of XIST impairs hypoxia-induced angiogenesis in HBMEC

This study firstly found that the expression levels of XIST were increased with hypoxia treatment in a time-dependent manner (**Figure 1A**). To assess the effects of XIST in HBMEC, the XIST gene was knocked down using specific siRNAs and the expression of XIST was verified by RT-qPCR assay (**Figure 1B**). Si-XIST#2 was chosen for the subsequent experiments. CCK8 analysis showed that knockdown of XIST under normal condition had no influence on cell proliferation. Hypoxia treatment could promote cell proliferation of HBMEC, while knockdown of XIST under hypoxia condition could inhibit cell proliferation (**Figure 1C**). We then investigate

the role of XIST on cell migration and angiogenesis under hypoxia stimulation. As expected, the results of showed that knockdown of XIST suppressed the HBMEC wound healing, transwell migration and tube formation caused by hypoxia stimulation (**Figure 1D-G**). These results suggested that knockdown of XIST suppressed hypoxia-induced angiogenesis.

XIST regulates SOX7 expression by sponging miR-485-3p in HBMEC

To explore the potential mechanism of XIST on angiogenesis, we investigated whether miRNAs participate in this process. StarBase v3.0 was used for bioinformatics analysis. As illustrated in **Figure 2A**, XIST contains a potential binding site for miR-485-3p. We then determined the expression of miR-485-3p in hypoxia-induced

XIST participate in hypoxia-induced angiogenesis

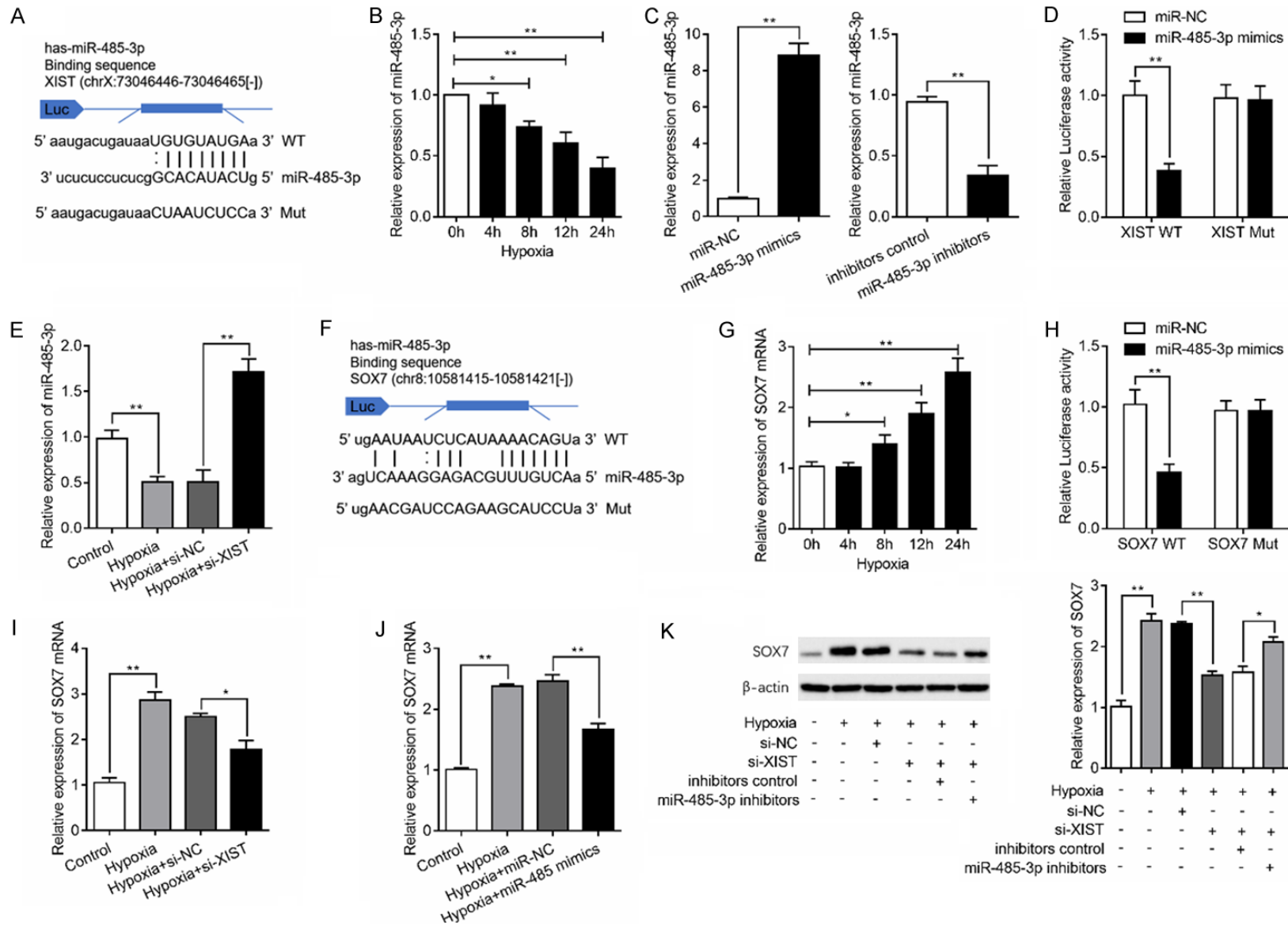


Figure 2. LncRNA XIST regulates SOX7 expression by sponging miR-485-3p. A. The schematic diagram shows the sequences of XIST 3'-UTR wild-type (WT) and mutant type (Mut), with miR-485-3p. B. Relative expression levels of miR-485-3p in HBMEC were determined by RT-qPCR under hypoxia stimulation for various time. C.

XIST participate in hypoxia-induced angiogenesis

Upregulation or downregulation of miR-485-3p was achieved by transfection with miR-485-3p mimics or inhibitors in HBMEC and the efficiency were validated by RT-qPCR. D. Luciferase reporter assay revealed the luciferase activity of XIST and miR-485-3p. E. HBMEC was transfected with si-NC or si-XIST and the expression of miR-485-3p was measured. F. The schematic diagram shows the sequences of SOX7 3'-UTR WT and Mut, with miR-485-3p. G. Relative expression levels of SOX7 were determined in HBMEC under hypoxia stimulation for various time. H. Luciferase reporter assay revealed the luciferase activity of miR-485-3p and SOX7. I. Relative expression of SOX7 mRNA in HBMEC with or without XIST silencing. J. HBMEC was transfected with miR-485-3p mimics, or miRNA negative controls (miR-NC) and SOX7 mRNA expression were measured. K. SOX7 protein levels was detected in HBMEC transfected with si-XIST, miR-485-3p inhibitors with or without hypoxia stimulation. *P<0.05, **P<0.01.

HBMEC and found miR-485-3p expression level was decreased with hypoxia stimulation in a time-dependent manner (**Figure 2B**). To determine the involvement of miR-485-3p in the role of XIST, upregulation and downregulation of miR-485-3p was achieved by transfected with miR-485-3p mimics and inhibitors, respectively (**Figure 2C**). Co-transfection with XIST-WT vector and miR-485-3p mimics reduced luciferase reporter activity when compared with the cells transfected with XIST-Mut (**Figure 2D**). In addition, XIST silencing significantly increased miR-485-3p expression under hypoxic condition (**Figure 2E**). Because miRNAs are known to target specific genes to regulate angiogenesis [19], we predicted the candidate gene of miR-485-3p using starBase v3.0 (**Figure 2F**). Our results showed that hypoxia stimulation caused significantly upregulation of SOX7 in a time-dependent manner (**Figure 2G**). Luciferase reporter analysis then validated the interaction between miR-485-3p and SOX7 (**Figure 2H**). Moreover, the results of RT-qPCR revealed that the expression of SOX7 was at least partly repressed after the knockdown of XIST (**Figure 2I**) or overexpression of miR-485-3p (**Figure 2J**) under hypoxia condition. Similarly, the results of western blot analysis showed that SOX7 protein levels was notably increased in HBMEC with hypoxia stimulation, while its level was decreased by knockdown of XIST. Inhibition of miR-485-3p partly reversed the inhibitory effects of XIST silencing on the expression of SOX7 proteins (**Figure 2K**). Taken together, XIST acts as an endogenous sponge by binding miR-485-3p, thus abolishing miR-485-3p-induced repression of SOX7.

XIST exerts its role via modulation of miR-485-3p/SOX7 axis in HBMEC under hypoxic condition

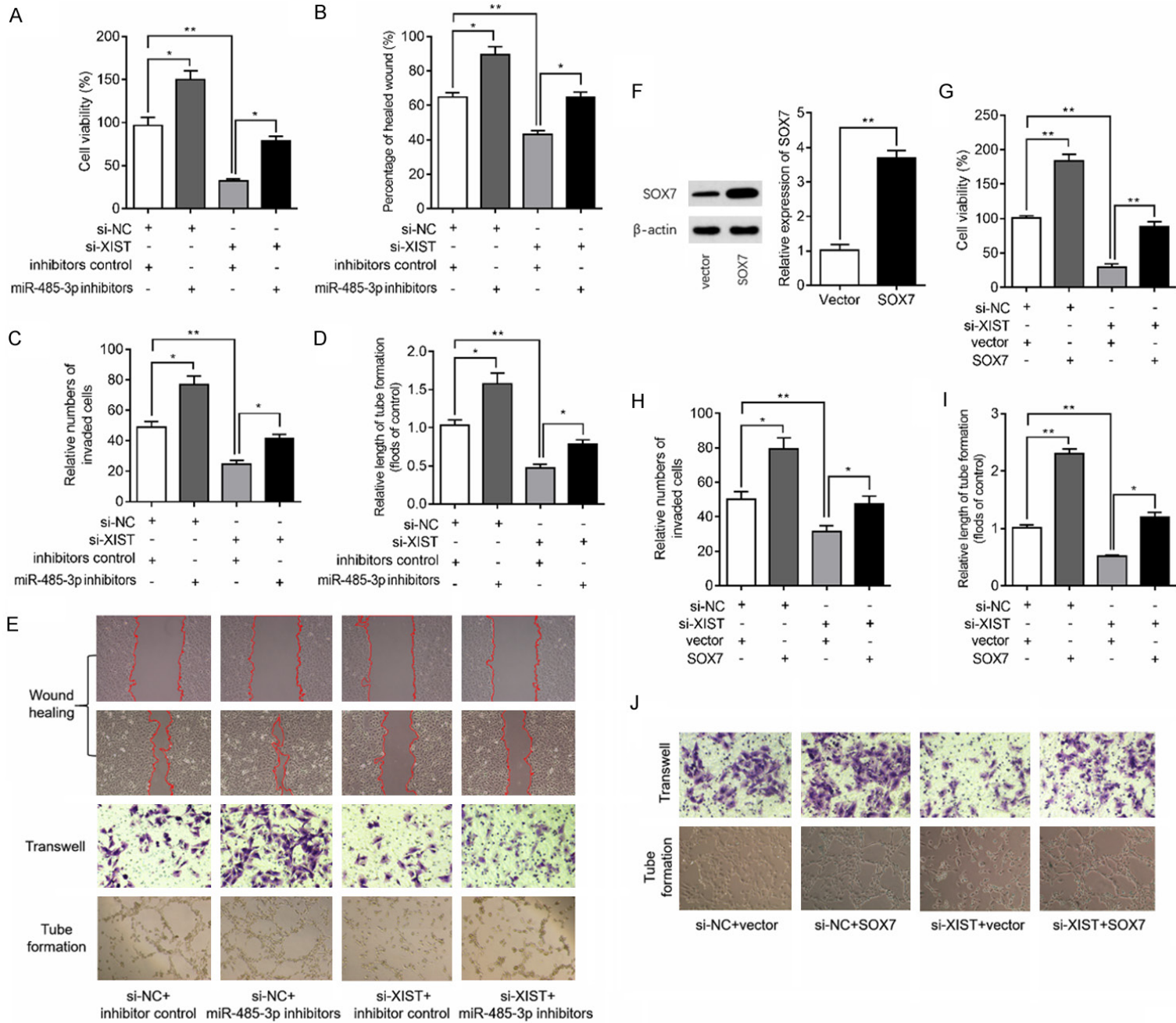
Based on the above findings that XIST regulates miR-485-3p/SOX7 axis, we then investigated whether the XIST affect the angiogenesis of HBMEC by regulation of miR-485-3p. Our find-

ings confirmed that inhibition of miR-485-3p lead to an increased cell proliferation of HBMEC under hypoxia condition and miR-485-3p inhibition could partly reverse the inhibitory effects of XIST silencing on cell proliferation in hypoxia-induced HBMEC (**Figure 3A**). Additionally, inhibition of miR-485-3p partially restores the wound healing (**Figure 3B** and **3E**), transwell migration (**Figure 3C** and **3E**) and tube formation (**Figure 3D** and **3E**) of HBMEC caused by XIST silencing under hypoxia condition. We then overexpressed of SOX7 by cell transfection to HBMEC with pcDNA3.1 plasmid carried SOX7 and the transfection efficiency was confirmed by western blot analysis (**Figure 3F**). Subsequent results of CCK8 assay, transwell assay and tube formation assay showed that overexpression of SOX7 caused notable enhanced proliferative ability of HBMEC under hypoxia condition and overexpression of SOX7 reversed the inhibitory effects of XIST silencing on cell proliferation (**Figure 3G**), migration (**Figure 3H** and **3J**), and angiogenesis (**Figure 3I** and **3J**) in hypoxia-induced HBMEC. These findings suggested that XIST participates in hypoxia-induced angiogenesis through miR-485-3p/SOX7 pathway.

XIST regulates VEGF signaling pathway through miR-485-3p/SOX7 axis in hypoxia-induced HBMEC

As the essential role of the VEGF signaling pathway during the angiogenesis [20] and the potential regulatory effects of SOX7 on VEGF pathway [21], we hypothesized that XIST promotes hypoxia-induced angiogenesis via the VEGF pathway. In addition, ERK and Akt pathway is the key intracellular signal transduction pathway for the angiogenesis after activation of VEGF signaling pathway [22], we also investigate the effects of XIST/miR-485-3p/SOX7 axis on the regulation of ERK and Akt pathway under hypoxia condition. As depicted in **Figure 4A**, hypoxia treatment for 24 h significantly upregulated the expression of VEGFR2 and VEGF, and

XIST participate in hypoxia-induced angiogenesis



XIST participate in hypoxia-induced angiogenesis

Figure 3. XIST exerts its role in HBMEC via regulation of miR-485-3p/SOX7 pathway. (A) HBMEC were exposed to siRNA negative control (si-NC) or si-XIST and/or to miR-485-3p inhibitors for 48 h and then subjected to hypoxia for 24 h, and then cell proliferation was measured using CCK8 kit. After the above indicated treatment, wound healing assay (B), transwell assay (C) and tube formation assay (D) were performed in HBMEC and the representative images were shown in (E). (F) HBMEC were exposed to control plasmid NC (vector) or SOX7 plasmid for 48 h, and Western blot analysis of the protein expression of SOX7 was qualified. (G) HBMEC were exposed to si-NC or si-XIST and/or to SOX7 plasmid for 48 h and then subjected to hypoxia for 24 h, and cell proliferation was determined by CCK8 kit. After the above indicated treatment, transwell assay (H) and tube formation assay (I) were performed in HBMEC and the representative images were shown in (J). * $P < 0.05$, ** $P < 0.01$.

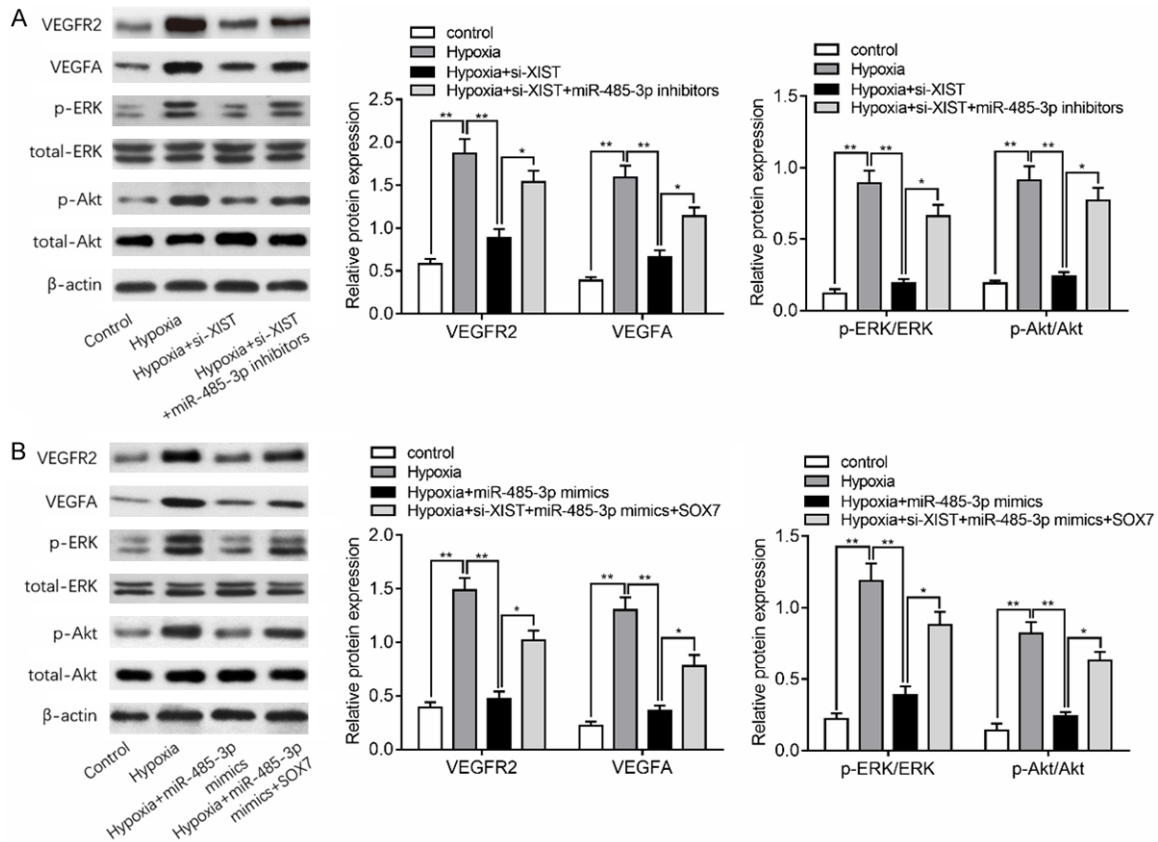


Figure 4. XIST regulates VEGF signaling in hypoxia-induced HBMEC. A. Western blots analysis showed the expression of VEGFR2 and VEGFA in HBMEC transfected with si-XIST and miR-485-3p inhibitors with or without hypoxia stimulation. Phosphorylation levels of the indicated kinases ERK1/2 and Akt were also quantified by densitometry and normalized to total kinase expression in above groups. B. VEGFR2 and VEGFA protein levels and ERK1/2 and Akt phosphorylation levels were shown in HBMEC transfected with miR-485-3p mimics and SOX7 plasmid. * $P < 0.05$, ** $P < 0.01$.

increased ERK1/2 and Akt phosphorylation. While silencing of XIST notably decreased the levels of VEGFR2 and VEGF, as well as ERK1/2 and Akt phosphorylation in response to hypoxia, which were partly reversed by inhibition of miR-485-3p. As shown in **Figure 4B**, upregulation of miR-485-3p decreased the protein expression of VEGFR2 and VEGFA, and inhibited ERK1/2 and Akt phosphorylation. However, overexpression of SOX7 could at least partly abolished this inhibitory effect of miR-485-3p on these factors. Collectively, our data demon-

strated that knockdown of XIST suppresses hypoxia-induced VEGF signaling pathway in HBMEC.

Discussion

The recovery from ischemic stroke largely relies on the appropriate restoration of blood flow via angiogenesis, which is a compensatory response to the reduction of oxygen [23, 24]. Angiogenesis is controlled by plenty of angiogenic factors and promoting angiogenesis

XIST participate in hypoxia-induced angiogenesis

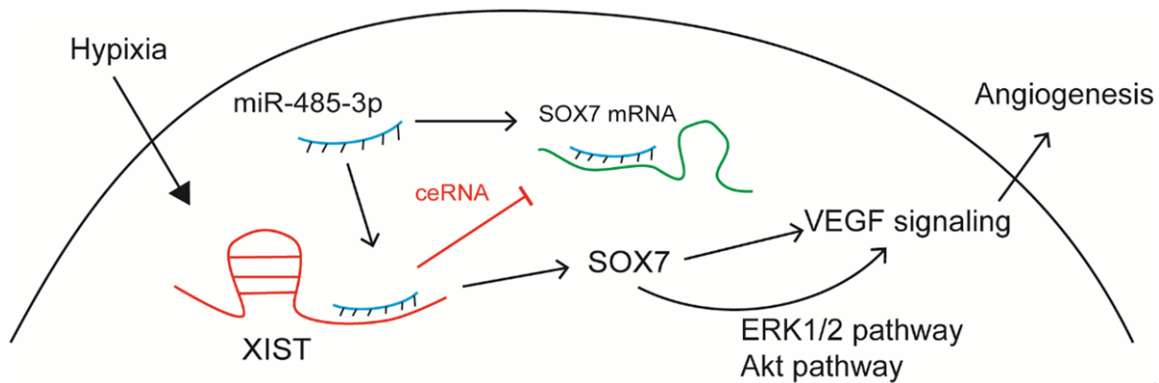


Figure 5. The function of lncRNA XIST in hypoxia-induced angiogenesis.

through various approaches that target angiogenic factors appears to be a useful treatment for experimental ischemic stroke [25]. In this study, we identified that lncRNA XIST levels in HBMEC increased with respect to hypoxia exposure time and knockdown of XIST suppressed the hypoxia-induced angiogenesis by regulation of miR-485-3p/SOX7/VEGF signaling pathway. It was the first time that the regulatory mechanism of XIST revealed in ischemic stroke and angiogenesis induced by hypoxia.

Convincing evidence suggests that XIST plays a vital role in the proliferation, migration, apoptosis and differentiation of human cells in a variety of cells [26, 27]. A recent study performed by Zhou et al found that XIST was upregulated in post-myocardial infarction myocardial cells and knockdown of XIST protected cell from myocardial infarction-induced cell death [28]. As well, Cheng et al. demonstrated that XIST silencing significantly inhibited glioma tumorigenicity and angiogenesis by targeting miR-429 [29]. More importantly, a recent study found that perfluorooctane sulfonate impaired normal placental angiogenesis by disrupting the lncRNA XIST-miR-429-VEGF-A pathway, inducing adverse fetal development [30]. Therefore, we hypothesized that XIST may also involve in hypoxia-induced angiogenesis. We found that XIST was significantly increased in hypoxia-induced HBMEC. Because endothelial cell proliferation and migration are both key steps involved in the angiogenic process [31], we investigated the effects of exogenous regulation of XIST on cell proliferative, migrative, as well as angiogenic capacity. With the finding that knockdown of XIST effectively suppressed cell proliferation, migration and angiogenesis under hypoxia condition, we suggested that

XIST participated hypoxia-induced angiogenesis.

However, the potential mechanism by which XIST exerted its role remains to be elucidated. Considering that plenty of studies have identified that lncRNAs can serve as a competing endogenous RNA to modulate the expression of miRNAs [32], we performed molecular experiments and bioinformatics analysis to further reveal the mechanisms underlying the action of XIST. A previous study showed that XIST could inhibit gastric carcinoma progression and metastasis by modulating the miR-101/EZH2 pathway [33]. Similarly, XIST integrated with miR-449 to regulate PTEN/PI3K/Akt signaling pathway to induce cell apoptosis in the pathogenesis of spinal cord injury [34]. Accordingly, our data demonstrated that XIST could bind 3'UTR of miR-485-3p to regulate SOX7 expression in HBMEC. Subsequently, we confirmed that inhibition of miR-485-3p or overexpression of SOX7 abolished the effects of XIST silencing on angiogenesis.

MiR-485-5p is identified as a tumor suppressor in various cancers, which is involved in multiple biological and pathological processes of cancers [35-37]. However, this is the first time showed miR-485-3p in involved in angiogenesis in hypoxia-induced endothelial cells. MiR-485-3p was found to target SOX7 to participate angiogenesis in our study. SOX7 is specifically expressed in the vascular endothelium and plays a critical role in vascular development [38]. SOX7 has a role in inducing and organizing the underlying vasculature development through producing vascular endothelial growth factor (VEGF) [39]. Our results also found that SOX7 overexpression could active VEGF signal-

XIST participate in hypoxia-induced angiogenesis

ing pathway, with the activation of ERK1/2 (necessary for tube formation) [40] and Akt (known to regulate cellular events required for new blood vessels formation) signaling. In addition, Kim even identified that SOX7 is an indispensable player in developmental angiogenesis by acting as positive feedback regulators of VEGF signaling [21]. Here, we showed XIST could regulate VEGF signaling, and other factors through regulation of miR-485-3p/SOX7 axis, thus to participate hypoxia-stimulated angiogenesis.

In summary, we firstly showed the participation of XIST in hypoxia-induced angiogenesis through regulation of SOX7 expression by sponging miR-485-3p (Figure 5). The data of this study would bring insight into XIST roles in angiogenesis and a further potential target for ischemic stroke.

Acknowledgements

This study was supported by the Applied Basic Research Project of Sichuan Province (2017JY0260).

Disclosure of conflict of interest

None.

Address correspondence to: Zhi Hu, Department of Critical Care Medicine, West China Hospital of Sichuan University, No 37, Guo Xue Xiang, Chengdu 610041, Sichuan, China. E-mail: hu_zwshsu@163.com

References

- [1] Cao R, Li J, Kharel Y, Zhang C, Morris E, Santos WL, Lynch KR, Zuo Z and Hu S. Photoacoustic microscopy reveals the hemodynamic basis of sphingosine 1-phosphate-induced neuroprotection against ischemic stroke. *Theranostics* 2018; 8: 6111-6120.
- [2] Saraiva JFK. Stroke prevention with oral anti-coagulants: summary of the evidence and efficacy measures as an aid to treatment choices. *Cardiol Ther* 2018; 7: 15-24.
- [3] Fluri F, Schuhmann MK and Kleinschnitz C. Animal models of ischemic stroke and their application in clinical research. *Drug Des Devel Ther* 2015; 9: 3445-3454.
- [4] Kong Q, Hao Y, Li X, Wang X, Ji B and Wu Y. HDAC4 in ischemic stroke: mechanisms and therapeutic potential. *Clin Epigenetics* 2018; 10: 117.
- [5] Spinelli C, Adnani L, Choi D and Rak J. Extracellular vesicles as conduits of non-coding RNA emission and intercellular transfer in brain tumors. *Noncoding RNA* 2018; 5.
- [6] Cui H, Liu T, Li P, Yang A, Zhou H, Luo J, Hu E, Hu W, Wang Y and Tang T. An intersectional study of LncRNAs and mRNAs reveals the potential therapeutic targets of buyang huanwu decoction in experimental intracerebral hemorrhage. *Cell Physiol Biochem* 2018; 46: 2173-2186.
- [7] Kumar MM and Goyal R. LncRNA as a therapeutic target for angiogenesis. *Curr Top Med Chem* 2017; 17: 1750-1757.
- [8] Bao MH, Szeto V, Yang BB, Zhu SZ, Sun HS and Feng ZP. Long non-coding RNAs in ischemic stroke. *Cell Death Dis* 2018; 9: 281.
- [9] Li L, Wang M, Mei Z, Cao W, Yang Y, Wang Y and Wen A. LncRNAs HIF1A-AS2 facilitates the up-regulation of HIF-1 α by sponging to miR-153-3p, whereby promoting angiogenesis in HUVECs in hypoxia. *Biomed Pharmacother* 2017; 96: 165-172.
- [10] Long FQ, Su QJ, Zhou JX, Wang DS, Li PX, Zeng CS and Cai Y. LncRNA SNHG12 ameliorates brain microvascular endothelial cell injury by targeting miR-199a. *Neural Regen Res* 2018; 13: 1919-1926.
- [11] Colognori D, Sunwoo H, Kriz AJ, Wang CY and Lee JT. Xist deletional analysis reveals an interdependency between Xist RNA and polycomb complexes for spreading along the inactive X. *Mol Cell* 2019; 74: 101-117, e10.
- [12] Liu X, Ming X, Jing W, Luo P, Li N, Zhu M, Yu M, Liang C and Tu J. Long non-coding RNA XIST predicts worse prognosis in digestive system tumors: a systemic review and meta-analysis. *Biosci Rep* 2018; 38.
- [13] Yildirim E, Kirby JE, Brown DE, Mercier FE, Sadyrev RI, Scadden DT and Lee JT. Xist RNA is a potent suppressor of hematologic cancer in mice. *Cell* 2013; 152: 727-742.
- [14] Xiao L, Gu Y, Sun Y, Chen J, Wang X, Zhang Y, Gao L and Li L. The long noncoding RNA XIST regulates cardiac hypertrophy by targeting miR-101. *J Cell Physiol* 2019; 234: 13680-13692.
- [15] Neumann P, Jae N, Knau A, Glaser SF, Fouani Y, Rossbach O, Kruger M, John D, Bindereif A, Grote P, Boon RA and Dimmeler S. The LncRNA GATA6-AS epigenetically regulates endothelial gene expression via interaction with LOXL2. *Nat Commun* 2018; 9: 237.
- [16] Xu X, Ma C, Liu C, Duan Z and Zhang L. Knockdown of long noncoding RNA XIST alleviates oxidative low-density lipoprotein-mediated endothelial cells injury through modulation of miR-320/NOD2 axis. *Biochem Biophys Res Commun* 2018; 503: 586-592.
- [17] Yu H, Xue Y, Wang P, Liu X, Ma J, Zheng J, Li Z, Li Z, Cai H and Liu Y. Knockdown of long non-coding RNA XIST increases blood-tumor barrier permeability and inhibits glioma angiogenesis

XIST participate in hypoxia-induced angiogenesis

- by targeting miR-137. *Oncogenesis* 2017; 6: e303.
- [18] Livak KJ and Schmittgen TD. Analysis of relative gene expression data using real-time quantitative PCR and the 2(-Delta Delta C(T)) Method. *Methods* 2001; 25: 402-408.
- [19] Qu M, Pan J, Wang L, Zhou P, Song Y, Wang S, Jiang L, Geng J, Zhang Z, Wang Y, Tang Y and Yang GY. MicroRNA-126 regulates angiogenesis and neurogenesis in a mouse model of focal cerebral ischemia. *Mol Ther Nucleic Acids* 2019; 16: 15-25.
- [20] Sadremontaz A, Mansouri K, Alemzadeh G, Safa M, Rastaghi AE and Asghari SM. Dual blockade of VEGFR1 and VEGFR2 by a novel peptide abrogates VEGF-driven angiogenesis, tumor growth, and metastasis through PI3K/AKT and MAPK/ERK1/2 pathway. *Biochim Biophys Acta Gen Subj* 2018; 1862: 2688-2700.
- [21] Kim K, Kim IK, Yang JM, Lee E, Koh BI, Song S, Park J, Lee S, Choi C, Kim JW, Kubota Y, Koh GY and Kim I. SoxF transcription factors are positive feedback regulators of VEGF signaling. *Circ Res* 2016; 119: 839-852.
- [22] Murakami M, Nguyen LT, Hatanaka K, Schachterle W, Chen PY, Zhuang ZW, Black BL and Simons M. FGF-dependent regulation of VEGF receptor 2 expression in mice. *J Clin Invest* 2011; 121: 2668-2678.
- [23] Krupinski J, Kaluza J, Kumar P, Kumar S and Wang JM. Role of angiogenesis in patients with cerebral ischemic stroke. *Stroke* 1994; 25: 1794-1798.
- [24] Greenberg DA. Cerebral angiogenesis: a realistic therapy for ischemic disease? *Methods Mol Biol* 2014; 1135: 21-24.
- [25] Yin KJ, Hamblin M and Chen YE. Angiogenesis-regulating microRNAs and ischemic stroke. *Curr Vasc Pharmacol* 2015; 13: 352-365.
- [26] Jiang H, Zhang H, Hu X and Li W. Knockdown of long non-coding RNA XIST inhibits cell viability and invasion by regulating miR-137/PXN axis in non-small cell lung cancer. *Int J Biol Macromol* 2018; 111: 623-631.
- [27] Engreitz JM, Pandya-Jones A, McDonel P, Shishkin A, Sirokman K, Surka C, Kadri S, Xing J, Goren A, Lander ES, Plath K and Guttman M. The Xist lncRNA exploits three-dimensional genome architecture to spread across the X chromosome. *Science* 2013; 341: 1237973.
- [28] Zhou T, Qin G, Yang L, Xiang D and Li S. LncRNA XIST regulates myocardial infarction by targeting miR-130a-3p. *J Cell Physiol* 2019; 234: 8659-8667.
- [29] Cheng Z, Li Z, Ma K, Li X, Tian N, Duan J, Xiao X and Wang Y. Long non-coding RNA XIST promotes glioma tumorigenicity and angiogenesis by acting as a molecular sponge of miR-429. *J Cancer* 2017; 8: 4106-4116.
- [30] Chen G, Xu LL, Huang YF, Wang Q, Wang BH, Yu ZH, Shi QM, Hong JW, Li J and Xu LC. Prenatal exposure to perfluorooctane sulfonate impairs placental angiogenesis and induces aberrant expression of lncRNA Xist. *Biomed Environ Sci* 2018; 31: 843-847.
- [31] Ucuzian AA, Gassman AA, East AT and Greisler HP. Molecular mediators of angiogenesis. *J Burn Care Res* 2010; 31: 158-175.
- [32] Cesana M, Cacchiarelli D, Legnini I, Santini T, Sthandier O, Chinappi M, Tramontano A and Bozzoni I. A long noncoding RNA controls muscle differentiation by functioning as a competing endogenous RNA. *Cell* 2011; 147: 358-369.
- [33] Chen DL, Ju HQ, Lu YX, Chen LZ, Zeng ZL, Zhang DS, Luo HY, Wang F, Qiu MZ, Wang DS, Xu DZ, Zhou ZW, Pelicano H, Huang P, Xie D, Wang FH, Li YH and Xu RH. Long non-coding RNA XIST regulates gastric cancer progression by acting as a molecular sponge of miR-101 to modulate EZH2 expression. *J Exp Clin Cancer Res* 2016; 35: 142.
- [34] Gu S, Xie R, Liu X, Shou J, Gu W and Che X. Long coding RNA XIST contributes to neuronal apoptosis through the downregulation of AKT phosphorylation and is negatively regulated by miR-494 in rat spinal cord injury. *Int J Mol Sci* 2017; 18.
- [35] Sun X, Liu Y, Li M, Wang M and Wang Y. Involvement of miR-485-5p in hepatocellular carcinoma progression targeting EMMPRIN. *Biomed Pharmacother* 2015; 72: 58-65.
- [36] Anaya-Ruiz M, Bandala C and Perez-Santos JL. miR-485 acts as a tumor suppressor by inhibiting cell growth and migration in breast carcinoma T47D cells. *Asian Pac J Cancer Prev* 2013; 14: 3757-3760.
- [37] Li J, Xu J, Yan X, Jin K, Li W and Zhang R. MicroRNA-485 plays tumour-suppressive roles in colorectal cancer by directly targeting GAB2. *Oncol Rep* 2018; 40: 554-564.
- [38] Nelson TJ, Chiriac A, Faustino RS, Crespo-Diaz RJ, Behfar A and Terzic A. Lineage specification of Flk-1+ progenitors is associated with divergent Sox7 expression in cardiopoiesis. *Differentiation* 2009; 77: 248-255.
- [39] Wat JJ and Wat MJ. Sox7 in vascular development: review, insights and potential mechanisms. *Int J Dev Biol* 2014; 58: 1-8.
- [40] Khalil A, Poelvoorde P, Fayyad-Kazan M, Rousseau A, Nuyens V, Uzureau S, Biston P, El-Makhour Y, Badran B, Van Antwerpen P, Boudjeltia KZ and Vanhamme L. Apolipoprotein L3 interferes with endothelial tube formation via regulation of ERK1/2, FAK and Akt signaling pathway. *Atherosclerosis* 2018; 279: 73-87.